Check for updates

ARTICLE

Identification of fusions with potential clinical significance in melanoma

Jakob M. T. Moran[1], Long P. Le[1], Valentina Nardi[1], Josephine Golas[1], Alexander A. Farahani [ID][1], Sylvia Signorelli[1], Maristela L. Onozato[1], Ruth K. Foreman[1], Lyn M. Duncan[1], Donald P. Lawrence[2], Jochen K. Lennerz [ID][1], Dora Dias-Santagata [ID][1,3 ✉] and Mai P. Hoang [ID][1,3 ✉]

Though uncommon in melanoma, gene fusions may have therapeutic implications. Next generation sequencing-based clinical assays, designed to detect relevant gene fusions, mutations, and copy number changes, were performed on 750 melanomas (375 primary and 375 metastases) at our institution from 2014–2021. These included 599 (80%) cutaneous, 38 (5%) acral, 11 (1.5%) anorectal, 23 (3%) sinonasal, 27 (3.6%) eye (uveal/ conjunctiva), 11 (1.5%) genital (vulva/penile), and 41 (5.5%) melanomas of unknown primary. Sixteen fusions (2%) were detected in samples from 16 patients: 12/599 (2%) cutaneous, 2/38 (5%) acral, 1/9 (11%) vulva, 1/23(4.3%) sinonasal; and 12/16 (75%) fusions were potentially targetable. We identified two novel rearrangements: *NAGS::MAST2* and *NOTCH1::GNB1*; and two fusions that have been reported in other malignancies but not in melanoma: *CANT1::ETV4* (prostate cancer) and *CCDC6::RET* (thyroid cancer). Additional fusions, previously reported in melanoma, included: *EML4::ALK, MLPH::ALK, AGAP3::BRAF, AGK::BRAF, CDH3::BRAF, CCT8::BRAF, DIP2B::BRAF, EFNB1::RAF1, LRCH3::RAF1, MAP4::RAF1, RUFY1::RAF1*, and *ADCY2::TERT*. Fusion positive melanomas harbored recurrent alterations in *TERT* and *CDKN2A*, among others. Gene fusions were exceedingly rare (0.2%) in *BRAF/RAS/NF1*-mutant tumors and were detected in 5.6% of triple wild-type melanomas. Interestingly, gene rearrangements were significantly enriched within the subset of triple wild-type melanomas that harbor *TERT* promoter mutations (18% versus 2%, $p < 0.0001$). Thirteen (81%) patients were treated with immunotherapy for metastatic disease or in the adjuvant setting. Six of 12 (50%) patients with potentially actionable fusions progressed on immunotherapy, and 3/6 (50%) were treated with targeted agents (ALK and MEK inhibitors), 2 off-label and 1 as part of a clinical trial. One patient with an *AGAP3::BRAF* fusion positive melanoma experienced a 30-month long response to trametinib. We show that, detecting fusions, especially in triple wild-type melanomas with *TERT* promoter mutations, may have a clinically significant impact in patients with advanced disease who have failed front-line immunotherapy.

INTRODUCTION

Melanoma accounts for the majority of deaths from skin cancers (9000 deaths per year) and its worldwide incidence is increasing[1,2]. Melanoma is often associated with cumulative solar damage from ultraviolet (UV) radiation, but it can occur at non-sun exposed anatomic locations, including mucosal, acral and uveal sites[1]. Treatment for melanoma ranges from surgical excision in cases of localized disease, to radiotherapy, chemotherapy, immunotherapy and targeted therapy in more complex or advanced cases[3]. Of special interest, are targeted agents that inhibit key pathways associated with melanoma carcinogenesis, such as the mitogen-activated protein kinase (MAPK) pathway, which involves the *KIT, NRAS, BRAF* and *MEK1/2* genes[4]. BRAF inhibitors such as Vemurafenib and Dabrafenib as well as MEK inhibitors such as Trametinib and Cobimetinib have been shown to improve survival outcomes[3]. Other kinase inhibitors such as Imatinib, Sunitinib, Dasatinib and Nilotinib may also have activity in patients with melanoma harboring *KIT* mutations[3].

The Tumor Cancer Genome Atlas (TCGA) has recognized four distinct subtypes of melanoma based on the molecular alteration present: mutant *BRAF*, mutant *RAS* (including *NRAS, KRAS* and *HRAS* genes), mutant *NF1* and a triple wild-type subtype (lacking hotspot mutations in *BRAF, NRAS, KRAS, HRAS* and *NF1*)[5]. *NF1* encodes a negative regulator of the RAS/MAPK pathway. Tumor suppressors *TP53, CDKN2A* and *PTEN* are often inactivated in all melanoma subtypes, by loss of function mutations or by whole gene deletion. Also frequently observed in melanomas, are *TERT* promoter mutations, which lead to increased expression of the *TERT* gene and to improved chromosomal stability in rapidly dividing cancer cells[6,7]. Ultraviolet radiation mutational signatures, resulting from cumulative solar damage and characterized by recurrent C to T transitions at the 3′ end of pyrimidine dimers, are commonly identified in cutaneous melanomas and associated with *TERT* promoter mutations[8]. While there is some overlap between the genetic signatures of cutaneous and mucosal melanomas, uveal melanomas are often characterized by mutations in *GNAQ/GNA11, BAP1, SF3B1*, and *EIF1AX*[4,9].

[1]Department of Pathology, Massachusetts General Hospital, Harvard Medical School, Boston, MA, USA. [2]Division of Medical Oncology, Department of Medicine, Massachusetts General Hospital Cancer Center, Harvard Medical School, Boston, MA, USA. [3]These authors contributed equally: Dora Dias-Santagata, Mai P. Hoang.
✉email: ddiassantagata@mgh.harvard.edu; mhoang@mgh.harvard.edu

Additionally, high-throughput, deep-sequencing technologies (next-generation sequencing) have allowed the identification of previously unknown alterations like gene fusions in a number of tumor types including sarcomas, carcinomas, gliomas and melanomas[10,11]. Some of these gene fusions are thought to function as driver mutations and the presence or absence of a gene fusion may enable risk stratification. Importantly, kinase fusions including genes such as *ALK*, *ROS*, *RET*, *NTRK* and *FGFR* family members have been identified in a variety of tumor types and can be targeted by available drugs[11].

Although gene fusions are rare in melanoma, rearrangements involving the *BRAF*, *RAF1*, *ALK*, *ROS1*, *NTRK1/2/3*, *MAP3K3*, *MAP3K8*, *PRKCA*, and *TRIM11* genes have been reported[11–16]. Interestingly, melanomas that contain kinase fusions have been reported to lack common driver mutations (*BRAF*, *NRAS*, *NF1*), further supporting the theory that gene rearrangements in melanoma represent driver mutations[14]. Identification of these driver mutations by next-generation sequencing may be clinically relevant if targeted therapy employed in other tumor types (e.g. *ALK* inhibitors in lung cancer) can be utilized in the treatment of melanoma[17]. In fact, in recent years, there have been several reports showing encouraging responses to specific inhibitors, in patients with fusion-associated melanomas[18–22].

Of note, gene fusions have been associated with distinct subtypes, morphologic patterns and particular anatomic sites. Kinase fusions occur in Spitz neoplasms and *BRAF* fusions are frequently documented in Spitz tumors[16,23]. Spitz tumors characteristically affect children and adolescents. Histopathologically they exhibit a dome-shaped or wedged-shaped proliferation associated with epidermal hyperplasia and junctional retraction artifact and are comprised of spindle tumor cells with abundant eosinophilic cytoplasm. While most Spitz tumors are benign, rare Spitz melanomas are asymmetric, typically lack dermal maturation, and have frequent mitotic figures, spindle morphology and severe cytologic atypia. In contrast, conventional melanomas exhibit an epithelioid morphology, i.e. the tumor cells are polygonal with abundant cytoplasm[24]. *BRAF* fusion-positive Spitz tumors have been reported to have epithelioid, high-grade morphology and *ALK* fusions have been detected in up to 13% of acral lentiginous melanomas[25,26]. These findings suggest gene fusions may play a role in tumorigenesis, histomorphologic patterns and may be site-specific.

In this study we report how our institution's approach of using next generation sequencing (NGS)-based assays for the clinical management of advanced cancer patients, resulted in the identification of rare and novel gene fusions in primary and metastatic melanomas from several anatomic sites (including cutaneous, anorectal, sinonasal, eye, genital and unknown site). Gene fusions were significantly enriched in triple wild-type melanomas harboring *TERT* promoter mutations (18%) and prompted the use of targeted therapies in 3 patients who progressed on immunotherapy, one of whom experienced a durable response to trametinib.

MATERIALS AND METHODS

Our study included 750 melanomas (375 primary and 375 metastases) submitted for clinical genetic profiling using targeted gene rearrangement testing and mutational analysis, from May 2014 until May 2021. Clinical parameters such as age, gender, treatment modality, and follow-up of the 16 patients whose tumors harbored fusions were collected from the patients' electronic medical records. The available histologic sections of fusion-positive tumors were reviewed to evaluate the histologic patterns including predominant cell morphology.

Molecular analyses

Tumor genotyping was performed using two types of clinically validated Anchored Multiplex PCR (AMP)-based NGS assays[27]. Gene fusions were identified using ribonucleic acid (RNA)-based assays, designed to detect fusion transcripts involving genes commonly rearranged in solid tumors (Supplementary Table 1). Briefly, total nucleic acid extracted from formalin-fixed paraffin-embedded (FFPE) tumors (after histological review for tumor enrichment), was reverse transcribed with random hexamers, and processed to create double stranded complimentary deoxyribonucleic acid (cDNA). Two hemi-nested polymerase chain reactions (PCR) were performed to create a fully functional sequencing library, using custom designed FusionPlex Solid Tumor kit primers (ArcherDx Inc., Boulder, CO, USA). Illumina NextSeq 2×150 base paired-end sequencing results were aligned to the hg19 human genome reference using bwa-mem[28]. A laboratory-developed algorithm was used for fusion transcript detection and annotation.

Clinically validated AMP-based assays (SNAPSHOT-NGS, V1 and V2) were used to detect single nucleotide variants (SNV), small insertion/deletions (indel), and copy number variants in genomic DNA (Supplementary Table 1). Genomic DNA extracted from FFPE tumor tissue was enzymatically sheared, end-repaired, adenylated, and ligated with a half-functional adapter. A sequencing library targeting hotspots and exons in 99 cancer genes was generated using two hemi-nested polymerase chain reactions and custom designed VariantPlex kit primers (ArcherDx Inc., Boulder, CO, USA). Illumina MiSeq 2×151 base paired-end sequencing results were aligned to the hg19 human genome reference using BWA-MEM (Li 2009). MuTect and a laboratory-developed insertion/deletion analysis algorithm were used for SNV and indel variant detection, respectively[29]. Tumor mutational burden (TMB) is reported as a total absolute count of somatic mutations (including intronic, synonymous and non-synonymous variants) across the covered regions of the SNAPSHOT-NGS-V2 assay (Supplementary Table 1). Upon clinical validation using orthogonal assays, an absolute TMB count greater than or equal to 15 was established as the reference range for TMB-High on this assay. The TMB scores reported in this study are specific to our SNAPSHOT-NGS-V2 NGS panel and direct conversion of the reported absolute TMB count to other assays or standards is not possible.

Fluorescence in-situ hybridization

Interphase dual color break apart fluorescence in-situ hybridization (FISH) was performed on select cases to confirm NGS Solid Fusion Assay results, as previously detailed[30]. *ALK* gene rearrangements were analyzed using the Vysis *ALK* break-apart probe FISH Probe Kit (Abbot Molecular, Des Plaines, IL). The *NOTCH1* rearrangement was confirmed using a commercially available *NOTCH1* break apart FISH probe (Empire Genomics, Williamsville, NY). *BRAF* gene rearrangements were evaluated using homebrew FISH probes, consisting of two BAC clones flanking the *BRAF* gene: RP11-715H9 (*BRAF* 5′, Spectrum Green) and RP11-248P7 (*BRAF* 3′, Spectrum Orange). Briefly, 5-micron sections of FFPE tumor material were baked, deparaffinized, and hybridized with FISH probes in a Hybrite slide processor (Abbott Molecular Inc., Abbott Park, IL, USA), according to the manufacturer's recommendations. After hybridization, the slides were washed, and the probes were visualized using an Olympus Bx61 microscope. FISH signals were evaluated in at least 50 nuclei in tumor-enriched areas, marked before slide processing, and the analysis was performed using the Cytovision software (Leica Biosystems, Buffalo Grove, IL, USA). A fused green-orange signal represents a normal gene. Fusion-positive nuclei show splitting of the green and orange probe signals further than two probes apart, in addition to the normal un-split green-orange signal. Samples were considered positive for a gene rearrangement, if more than 15% of scored tumor cells had split 5′ and 3′ FISH probe signals.

Immunohistochemistry and immunofluorescence

Immunohistochemical studies were performed on 5-micrometer-thick tissue sections using a Bond 3 automated immunostainer (Leica Microsystems, Bannockburn, IL, USA), with primary antibodies against ALK (predilute, 5 A4, Leica Microsystems) and Notch1 (D1E11, Cell Signaling Technology, Danvers, MA). Immunofluorescence studies were performed manually on 5-micrometer-thick tissue sections using standard protocol with primary antibodies against MAST2 (1:100, HPA039722, Sigma Aldrich, St. Louis, MA) and GNB1 (1:200, SAB2701168, Sigma Aldrich) and secondary antibodies (anti rabbit, Alexa Fluor 647 (cy5), 1:300, Thermo Fisher Scientific, Waltham, MA for MAST2; Goat anti rabbit, Alexa Fluor™ Plus 594, A32740, Thermo Fisher Scientific for GNB1).
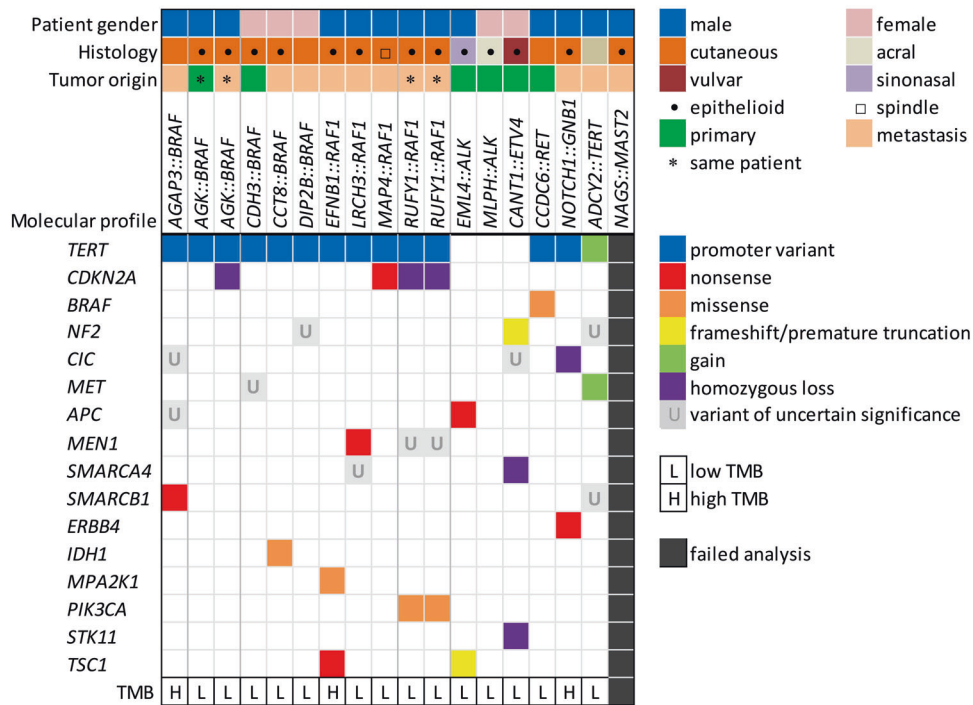
Fig. 1 Summary of fusion and next generation sequencing results of the fusion-positive cases. There was no evidence of loss of heterozygosity (LOH) for genes affected by nonsense or frameshift mutations.

RESULTS

Molecular analyses

Sixteen gene fusions were detected in 6 primary tumors and in 12 metastases of 16 patients (Fig. 1, Table 1). The presumed mechanisms underlying these fusions include translocation (7 cases), inversion (7 cases), and deletion (2 cases) (Table 1). Using public databases (COSMIC and TCGA) and published literature (PubMed) we identified 4 novel fusions, including 2 that have been reported in other malignancies but not in melanomas: CANT1::ETV4 (prostate cancer), CCDC6::RET (thyroid cancer), and 2 fusions that, to our knowledge, have not been previously described: NAGS::MAST2 and NOTCH1::GNB1 (Table 1, Fig. 2). The NOTCH1 rearrangement juxtaposes NOTCH1 exon 2 to the 5′-UTR of GNB1, immediately upstream of the GNB1 starting codon, and it does not appear to generate an in-frame chimeric protein between NOTCH1 and GNB1. However, it may function by inactivating NOTCH1, and/or by driving GNB1 expression under the control of the NOTCH1 promoter.

Additional fusions involving ALK (EML4::ALK, MLPH::ALK), BRAF (AGAP3::BRAF, AGK::BRAK, CDH3::BRAF, CCT8::BRAF, DIP2B::BRAF), RAF1 (EFNB1::RAF1, LRCH3::RAF1, MAP4::RAF1, RUFY1::RAF1), and TERT (ADCY2::TERT) have been previously reported in melanomas[11–15,17,23,25,26].

Mutational analyses were successfully performed in samples from 15/16 patients with fusion-positive melanomas (Supplementary Table 2). For 2 patients, molecular testing was done on two available samples, and the same fusion and similar mutational profiles were detected in each specimen (Fig. 1). In one patient, the same AGK::BRAF fusion was detected in the primary tumor and in a bone metastasis resected one month later (Table 1, case 2). The two specimens were positive for the same mutations in NF1, KDR and in the TERT promoter, and the bone metastasis also showed homozygous loss of CDKN2A (Fig. 1, Supplementary Table 2). In another patient, the same RUFY1::RAF1 fusion was detected in two different metastases (lung and bone) that were resected 9 months apart (Table 1, case 9), and the two samples

harbored the same mutations in PIK3CA, MEN1 and in the TERT promoter, and homozygous deletion of CDKN2A (Fig. 1, Supplementary Table 2). Fusion positive melanomas harbor oncogenic mutations in genes involved in receptor tyrosine kinase, MAPK/ERK, and mTOR signaling pathways (including ERBB4, MET, MAP2K1, PIK3CA, STK11, and TSC1). The most prevalent genetic abnormalities detected in our fusion-positive cohort involved the TERT gene (Fig. 1), and included 11/15 (73%) cases with hotspot mutations in the TERT promoter (C250T, 6 cases; C228T, 5 cases) and a TERT gene amplification in the sample harboring the ADCY2::TERT fusion (case 15). TERT promoter mutations were detected in 63% of fusion negative melanomas, and we found no significant association between the presence of a TERT promoter mutation and fusion positivity ($p = 0.59$) (Supplementary Table 3). Pathogenic mutations in CDKN2A, especially homozygous gene deletion, were the second most common finding, being detected in 3/15 (20%) patients with fusion-positive melanoma (Fig. 1). Gene fusions were largely mutually exclusive from mutations in the most common oncogenic drivers in melanoma. Pathogenic mutations in RAS (NRAS, KRAS or HRAS) family members, NF1 or KIT were absent from fusion-positive cases, while fusion-negative melanomas harbored mutations in all of them, at the following frequencies: 28% NRAS[mut], 31% RAS (NRAS, KRAS or HRAS)[mut], and 6% KIT[mut]. BRAF mutations were detected in 37% of fusion-negative melanomas and in 1/15 (7%) fusion positive cases.

There was a highly significant association between the presence of fusions and the absence of BRAF/RAS mutation ($p < 0.00001$, Supplementary Table 3), with gene fusions being detected in 5.4% of BRAF and RAS wild-type melanomas, and only in 0.2% of BRAF-mutant or RAS-mutant tumors. Our cohort included 166 (23%) triple wild-type melanomas. Interestingly, while TERT promoter mutations were very prevalent in fusion positive melanomas (11 of 15, 73%) and in BRAF/NRAS/NF1-driven cases (393 of 542, 73%), they were underrepresented in triple wild-type melanomas (56 of 166, 34%). Therefore, while gene fusions are very rare in melanoma (16 of 708, 2% in our cohort), they were significantly enriched within the subset

Table 1. Summary of molecular, clinical and histologic findings of 16 fusion-positive cases.

	Rearrangement/ Fusion[a] Fusion partners (transcripts)	Fusion mechanism[b]	TMB (score)	Site of tested specimen	Melanoma subtype[c] histology of primary	Age (years)/ Gender	Clinical stage[d]	Treatment	Outcome followup
1	AGAP3::BRAF AGAP3 exon 10 BRAF exon 6	Inversion	High (27)	Metastasis, chest wall skin	Cutaneous Nodular, Clark level IV, depth 1.95 mm, non-ulcerated, mitoses >6/mm²	42/M	III	Surgery; Radiation IT: Pembro TT: Trametinib[CT], MEK[inhib] IS: *Infliximab, Prednisone*	AWD 116 mo
2	AGK::BRAF AGK exon 2 BRAF exon 8	Inversion	Low (13)	Primary, right shoulder Metastasis, right scapula	Cutaneous NOS, epithelioid, Clark level IV, depth at least 8.0 mm, ulcerated, 46 mitoses per mm²	45/M	IV	IT: Ipi/Nivo IS: *Prednisone*	NED 23 mo
3	CDH3::BRAF CDH3 exon 15 BRAF exon 6	Translocation	Low (7)	Primary, left posterior shoulder	Cutaneous NOS, epithelioid, Clark level IV, depth 3.9 mm, ulcerated, 10 mitoses per mm²	76/F	IIB	Surgery	NED 13 mo
4	CCT8::BRAF CCT8 exon 14 BRAF exon 9	Translocation	Low (11)	Metastasis, left chest skin	Cutaneous Nodular, epithelioid, Clark level IV, 1.67 mm, ulcerated	53/F	IIA	Surgery; Radiation; Cryotherapy[CT] IT: IFN[CT] (adjuvant), Nivo/TAK-202[CT], Pembro, Ipi IS: *Prednisone, Methylprednisolone*	DOD 47 mo
5	DIP2B::BRAF DIP2B exon 19 BRAF exon 9	Translocation	Low (6)	Metastasis, inguinal lymph node	Cutaneous NM, epithelioid, Clark level IV, depth 1.4 mm, non-ulcerated, 5 mitoses per mm²	56/F	III	IT: Pembro, Nivo/anti-LAG3 mAb[CT], Ipi IS: *Infliximab, Methylprednisolone, Prednisone*	DOD 14 mo
6	EFNB1::RAF1 EFNB1 exon 5 RAF1 exon 9	Translocation	High (16)	Metastasis, brain	Cutaneous SSM, epithelioid, Clark level IV, depth 2.75 mm, non-ulcerated, 0 mitoses per mm²	56/M	IIA	Surgery IT: Ipi/Nivo IS: *Methylprednisolone, Infliximab, Prednisone, Vedolizumab*	DOD 58 mo
7	LRCH3::RAF1 LRCH3 exon 12 RAF1 exon 9	Inversion	Low (13)	Metastasis, brain	Cutaneous SSM, epithelioid, Clark level III, depth 0.45 mm, not ulcerated, 2 mitoses per mm²	73/M	IV	Surgery; Radiation IT: Pembro	AWD 12 mo
8	MAP4::RAF1 MAP4 exon 13 RAF1 exon 8	Deletion	Low (12)	Metastasis, lung	Cutaneous SSM, spindle, Clark level IV, depth of 0.62 mm, non-ulcerated, 3 mitoses per mm²	50/M	IA	Surgery IT: Pembro (adjuvant/ neoadjuvant)	NED 173 mo
9	RUFY1::RAF1 RUFY1 exon 9 RAF1 exon 10	Translocation	Low (12)	Metastasis, lung Metastasis, brain	Cutaneous NM, epithelioid, Clark level IV, depth of 1.65 mm, non-ulcerated, 3 mitoses per mm²	51/M	III	Surgery IT: Pembro, Ipi/ Nivo TT: Binimetinib, MEK[inhib] IS: *Methylprednisolone, Infliximab*	DOD 40 mo
10	EML4::ALK EML4 exon 5 ALK exon 20	Inversion	Low (11)	Primary, nasopharynx	Mucosal, Sinonasal Epithelioid, depth 4 mm, ulcerated, 3 mitoses per mm²	59/M	IIB	Surgery; Radiation IT: Ipi/Nivo[CT], Nivo/T-VEC TT: Alectinib, ALK inhibitor Chemotherapy: Carbo/Taxol Cell therapy: TCR-engineered T cells against the MAGE-A3/A6 antigens IS: *Prednisone, Infliximab*	DOD 41 mo
11	MLPH::ALK MLPH exon 12 ALK exon 20	Inversion	Low (9)	Primary, left foot	Acral ALM, epithelioid, Clark level IV, depth 1 mm, non-ulcerated, 2 mitoses per mm²	29/F	III	Surgery IT: IFN (adjuvant)	NED 53 mo

Table 1. continued

	Rearrangement/ Fusion[a] Fusion partners (transcripts)	Fusion mechanism[b]	TMB (score)	Site of tested specimen	Melanoma subtype[c] histology of primary	Age (years)/ Gender	Clinical stage[d]	Treatment	Outcome followup
12	CANT1::ETV4 novel in melanoma CANT1 exon 3 ETV4 exon 7	Deletion	Low (6)	Primary, vulva	Mucosal MLM, epithelioid, Clark level IV, depth 6 mm, ulcerated, 16 mitoses per mm², lymphovascular invasion present	82/F	IIC	Surgery; Radiation IT: Pembro	DOD 20 mo
13	CCDC6::RET novel in melanoma CCDC6 exon 1 RET exon 12	Inversion	Low (12)	Primary, right knee	Cutaneous SSM, epithelioid, Clark level IV, depth 2.3 mm, non-ulcerated, 15 mitoses per mm²	72/M	III	Surgery	NED 25 mo
14	NOTCH1::GNB1[e] novel NOTCH1 exon 2 GNB1 exon 2	Translocation	High (23)	Metastasis, intraparotid lymph node	Cutaneous - NA Metastasis - epithelioid	55/M	III	Surgery; Radiation IT: Pembro, Ipi/Nivo IS: Prednisone (s/p kidney transplant)	AWD 53 mo
15	ADCY2::TERT ADCY2 exon 20 TERT exon 2	Inversion	Low (13)	Metastasis, lung	Acral NOS, epithelioid and spindle, Clark level IV, depth of 1.9 mm, ulcerated, 8 mitoses per mm²	58/M	III	Surgery; Radiation; Cryotherapy[CT] IT: Ipi (adjuvant)[CT], Pembro IS: Prednisone, Budesonide	AWD 73mo
16	NAG::MAST2 novel NAGS exon 6 MAST2 exon 5	Translocation	N/A	Metastasis, neck lymph node	Cutaneous NOS, epithelioid, Clark level IV, depth of 4.9 mm, non-ulcerated, 6 mitosis per mm²	56/M	III	Surgery IT: Nivo (adjuvant)	NED 42 mo

AWD alive with disease, *NED* no evidence of disease, *DOD* died of disease, *N/A* not available, *M* male, *F* female, *mo* months, *inhib* inhibitor, *IT* immunotherapy/immuno checkpoint inhibitors, *TT* targeted therapy, *IS* immunosuppressants, *Pembro* Pembrolizumab, *Ipi* Ipilimumab, *Nivo* Nivolumab, *IFN* interferon, *CT* clinical trial, *MLM* mucosal lentiginous melanoma, *SSM* superficial spreading melanoma, *NM* nodular melanoma, *ALM* acral lentiginous melanoma, *LMM* lentigo maligna melanoma, *NOS* unclassified.

[a]Potentially targetable fusions are shown in bold.

[b]When the two partners are on the same chromosome, the presumed fusion mechanisms are inversions or deletions, depending on the orientation of their coding sequences. However, these fusions could result from more complex rearrangements.

[c]In addition to melanoma, patient 6 had mantle cell lymphoma and patient 13 had thymoma.

[d]Clinical stage at presentation, according to the 8th edition of the American Joint Committee on Cancer (AJCC) melanoma staging system (2018).

[e]The *NOTCH1::GNB1* rearrangement is not expected to produce a chimeric fusion protein involving *NOTCH1* and *GNB1*. Instead, as detailed in the text, this rearrangement may activate expression of the full-length GNB1 protein, under the control of the *NOTCH1* promoter.
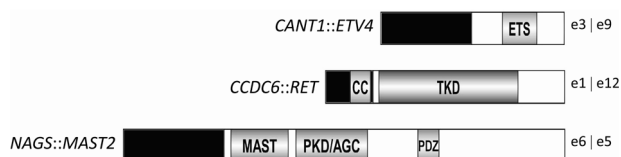
Fig. 2 Schematic representation of three fusions not previously reported in melanoma. The *NAGS::MAST2* fusion has not been previously reported in the literature. The other two fusions have been described in other malignancies but not in melanoma: *CANT1::ETV4* in prostate cancer and *CCDC6::RET* in thyroid cancer. The putative chimeric proteins are depicted with the N-terminal fusion partner shown in black, and the C-terminal partner in white. The exon breakpoints, listed on the right, are based on the following transcripts: *CANT1* (ENST00000392446.5); *ETV4* (ENST00000319349.5); *CCDC6* (ENST00000263102.6); *RET* (ENST00000355710.3); *NAGS* (ENST00000293404.3); *MAST2* (ENST00000361297.2). Relevant functional domains: DNA binding domain (ETS: erythroblast transformation specific), kinase domains (TKD: tyrosine kinase domain; MAST: microtubule-associated serine-threonine kinase; PKD: protein kinase domain; AGC: cAMP-dependent, cGMP-dependent and protein kinase C kinase C-terminal), WD: WD (tryptophan and aspartic acid) repeat domains, CC: coiled coil homodimerization domain; PDZ: PSD-95, Dlg1, Zo-1 protein interaction domain. The *NOTCH1::GNB1* rearrangement, which has not been previously reported in the literature, was excluded from this figure because it is not expected to lead to the production of an in-frame chimeric fusion protein involving *NOTCH1* and *GNB1*. As noted in the text, this rearrangement may result in the expression of the full length GNB1 protein under the control of the *NOTCH1* promoter.

of triple wild-type melanomas that harbor *TERT* promoter mutations (10 of 56, 18%, $p < 0.00001$, Supplementary Table 3).

Tumor mutational burden (TMB) was available for 412 cases. In our cohort, 48% (189 of 397) of fusion-negative tumors had a high TMB, while only 20% (3 of 15) of fusion-positive melanomas were found to have a high TMB (Table 2). High TMB cases included three cutaneous melanomas, positive for *BRAF*, *RAF1* and *NOTCH1* fusions (Table 1, cases 1, 6, and 14, respectively). Interestingly, for the 2 cases with very high TMB scores (cases 1 and 14, with TMB > 20), C > T transitions accounted for 73–78% of the mutations, a pattern consistent with exposure to UV radiation.

Fluorescence in situ hybridization, immunohistochemistry and immunofluorescence studies
Selected rearrangements were confirmed by orthogonal assays. A commercially available *NOTCH1* break apart FISH probe detected a *NOTCH1* rearrangement in the melanoma sample harboring the novel *NOTCH1::GNB1* fusion (case 14). The *CDH3::BRAF* and *CCT8::BRAF* fusions were confirmed by *BRAF* break apart FISH, and the *EML4::ALK* and *MLPH::ALK* rearrangements were validated by *ALK* break apart FISH (Fig. 3).

ALK immunostain performed on the melanoma harboring the *EML4::ALK* fusion (case 10) was positive for ALK expression (Fig. 4). To evaluate the effects of previously unreported rearrangements, we performed immunoassays on fusion-positive melanomas and on a fusion-negative melanoma harboring a *BRAF* V600E mutation, which is the most common genetic alteration observed in these tumors (Fig. 5). We also assessed publically available datasets, to examine protein expression levels across multiple melanomas (Supplementary Figs. 1–3). Notch1 immunostaining demonstrated that the melanoma sample harboring the *NOTCH1::GNB1* rearrangement (case 14) was positive for Notch1 expression (Fig. 5A), and that Notch1 protein levels were comparable to the ones observed in a *BRAF* V600E-mutant melanoma (Fig. 5B). Data from The Human Protein Atlas demonstrated weak (6 of 12) and moderate (6 of 12) Notch1 expression across 12 melanoma samples, with most cases (11 of 12) exhibiting a cytoplasmic/membranous and nuclear distribution of the protein (Supplementary Fig. 1).

Immunofluorescence staining using a GNB1-specific antibody demonstrated uniform cytoplasmic and membranous GNB1 expression in the *NOTCH1::GNB1* positive melanoma (case 14) (Fig. 5C), and heterogeneous distribution of *GNB1* in a *BRAF* V600E-mutant melanoma (Fig. 5D). GNB1 immunostaining, made available by The Human Protein Atlas, showed variable levels of cytoplasmic/membranous GNB1 expression across 11 melanomas, ranging from moderate (4 of 11) and weak (3 of 11), to no detectable levels in 4 of 11 cases (Supplementary Fig. 2). Immunofluorescence analysis using a MAST2-specific antibody showed similar patterns of heterogeneous expression of MAST2 in the melanoma sample harboring a *NAGS::MAST2* rearrangement (case 16) (Fig. 5E) and in a *BRAF* V600E-mutant melanoma (Fig. 5F). MAST2 immunostaining results from The Human Protein Atlas, demonstrated variable levels of cytoplasmic/membranous MAST2 in 12 melanomas, with most cases showing moderate (3 of 12) or weak (5 of 12) expression, and 4 of 12 cases being negative for MAST2 (Supplementary Fig. 3).

Clinical and histological features
The primary tumor site of all analyzed melanomas included 599 (80%) cutaneous, 38 (5%) acral, 11 (1.5%) anorectal, 23 (3%) sinonasal, 27 (3.6%) eye (uveal/conjunctiva), 11 (1.5%) genital (vulva/penile), and 41 (5.5%) cases of unknown primary. Within the fusion-positive cohort, 12/599 (2%) melanomas were cutaneous, 2/38 (5%) acral, 1/9 (11%) vulvar, and 1/23 (4.3%) sinonasal (Table 1). *MLPH::ALK* and *ADCY2::TERT* fusions involved the acral site, *CANT1::ETV4* the vulva, *EML4::ALK* the sinonasal region, and the remaining fusions were detected in in tumors from cutaneous sites. We found no significant difference between the prevalence of fusions in cutaneous (2.2%) versus non-cutaneous (3.6%) sites (Supplementary Table 3).

The sites of the 12 metastases were lung (3), lymph node (3), bone (2), brain (2), skin (1) and soft tissue (1). Overall, there were 438 males and 312 females, including 427/734 (58%) males with fusion-negative tumors and 11/16 (69%) male patients with fusion positive melanomas. There was no significant association between gender and fusion positivity (Supplementary Table 3). The age at diagnosis ranged from 29 to 83 years (median, 56 years). Two (12.5%) patients presented with stage IV disease (distant metastases), 8 (50%) with stage III (nodal involvement), 5 (31%) with stage II, and 1 (6%) patients with stage I melanoma (Table 1)[31].

The majority of fusion positive cases (92%, 12 of 13) exhibited an epithelioid morphology, with only one tumor (positive for a *MAP4::RAF1* fusion) demonstrating spindle cell morphology (Fig. 4). Surgical specimens were available for histopathological review in 4 out of 5 *BRAF* fusion-positive melanomas, and none of them exhibited a spindled morphology.

Treatment and outcome
Fifteen of 16 patients (94%) underwent surgery, primarily for the treatment of localized disease (to excise the primary tumor and nodal metastases). Two patients received surgery alone and have no evidence of disease after 13 and 25 months. Seven patients were treated with radiotherapy. Two patients enrolled in clinical trials using cryoablation to target metastases.

Thirteen (81%) patients were treated with immunotherapy for metastatic disease or in the adjuvant setting. Nine and eight patients received the PD-1 inhibitors pembrolizumab and nivolumab, respectively and nine patients received anti-CTLA-4 therapy (ipilimumab). Nivolumab was often used in combination with other agents (on 6 occasions with ipilimumab, and once with: CCR2 antagonist TAK-202, anti-LAG3 antibody, and T-VEC oncolytic virus). Nine patients received immunosuppressive treatment, in most cases, to manage serious adverse events associated with immune checkpoint inhibitor therapy.

Table 2. Distribution of fusion positive and fusion negative melanomas, according to patient gender, tumor mutational burden, prevalence of oncogenic mutations, and tumor type.

	N			Fusion positive (%)	Fusion negative (%)
Gender	750	Male		11 (69)	427 (58)
		Female		5 (31)	307 (42)
Tumor mutational burden	412	High		3 (20)	189 (48)
		Low		12 (80)	208 (52)
TERT promoter mutation	708	Positive		11 (73)	438 (63)
		negative		4 (27)	255 (37)
BRAF mutation	708	Positive		1 (7)	259 (37)
		Negative		14 (93)	434 (63)
NRAS mutation	708	Positive		0 (0)	194 (28)
		Negative		15 (100)	499 (72)
BRAF or *RAS* mutation (*NRAS/KRAS/HRAS*)	708	Positive		1 (7)	448 (65)
		Negative		14 (93)	245 (35)
Triple wild type *and TERT* promoter mutation	708	Positive		10 (67)	46 (7)
		Negative		5 (33)	647 (93)
Tumor type	708	Cutaneous		12 (75)	587 (85)
		Non-cutaneous		4 (25)	105 (15)

ALK break apart FISH   *BRAF* break apart FISH
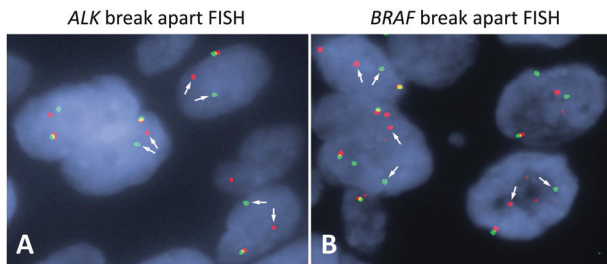
Fig. 3 *ALK* and *BRAF* break apart fluorescence in situ hybridization. Fluorescence in-situ hybridization using break-apart probes for (**A**) *ALK* (case 9, *MLPH::ALK*) and (**B**) *BRAF* (case 4, *CCT8::BRAF*). Fusion-positive nuclei show splitting of the green and orange probe signals further than two probes apart (arrows), in addition to the normal unsplit green-orange signal.

Six of 12 (50%) patients with potentially actionable fusions progressed on immunotherapy, and 3/6 (50%) were treated with targeted agents (ALK and MET inhibitors), 2 off-label and 1 as part of a clinical trial. One patient with an *AGAP3::BRAF* fusion positive melanoma experienced a 30-month long response to trametinib. Another patient whose tumor harbored a *RUFY1::RAF1* fusion was placed on binimetinib, a MEK inhibitor. Treatment only lasted four months, as the patient experienced a mixed response to this MEK inhibitor, with major response to therapy in his visceral organs but marked progression in his bone metastases. One patient whose melanoma harbored an *EML4::ALK* fusion received an ALK inhibitor (alectinib), but experienced disease progression after one month (Table 1). Follow-up since time of diagnosis ranges from 12 months to 173 months (median, 41 months). Six patients died and ten are alive (4 with disease and 6 with no evidence of disease) (Table 1).

DISCUSSION
We identified 4 novel fusions, including 2 that have been reported in other malignancies but not in melanoma (*CANT1::ETV4* and *CCDC6::RET*) and 2 fusions that have not been described in the literature (*NAGS::MAST2* and *NOTCH1::GNB1*). A *CANT1::ETV4* fusion was detected in one primary vulvar melanoma in our series. To date, *CANT1::ETV4* fusion has only been reported in prostate carcinoma[32]. *ETV4* belongs to the family of ETS-related transcription factors and has been reported as a rare fusion partner of *EWSR1* in classical Ewing sarcoma[33]. Calcium-activated nucleotidase 1 (CANT1) expression is regulated by androgen and its exon 1a transcript is preferentially expressed in the prostate[32]. A *CCDC6::RET* fusion was detected in a primary melanoma from the lower extremity in our series. The same fusion between *CCDC6* exon 1 and *RET* exon 12 has been previously documented in papillary thyroid carcinoma, but not in melanoma[34]. *NAGS::MAST2* and *NOTCH1::GNB1* rearrangements, identified in two metastatic melanomas in our series, have not been reported in any malignancies. Recurrent rearrangements of the microtubule associated serine-threonine (MAST) kinase and *NOTCH* gene families have been reported in breast cancer[35]. Breast cancer cell lines harboring *NOTCH* rearrangements have been shown to exhibit sensitivity to inhibition of Notch signaling[35]. In addition, overexpression of *MAST1* or *MAST2* fusions had a proliferative effect on tumor cells[35].

Our sequencing results do not support the production of an in-frame *NOTCH1::GNB1* chimeric protein, suggesting that (in contrast to the fusions reported in breast cancer) this rearrangement may result in loss of function of *NOTCH1*. Interestingly, immunohistochemistry showed that the presence of this rearrangement does not seem to reduce Notch1 protein levels in the *NOTCH1::GNB1*-positive tumor, when compared to a BRAF V600E-positive melanoma (Fig. 5A, B). The results suggest that, although the rearrangement may inactivate one copy of *NOTCH1*, it does not appear to significantly impact *NOTCH1* activity in this tumor (presumably because the second allele remains intact). As noted, the *NOTCH1* rearrangement juxtaposes *NOTCH1* exon 2 immediately upstream of the *GNB1* starting codon and it could, potentially, drive *GNB1* expression under the control of the *NOTCH1* promoter. *GNB1* encodes the beta subunit of a trimeric G protein complex that mediates signaling downstream of G-protein coupled receptors. Previous research showed that *GNB1* is activated by recurrent somatic mutations in hematopoietic malignancies and in solid tumors, including melanoma[36]. A recent study showed that GNB1 is overexpressed in a subset of cervical squamous cell carcinomas, with high levels of GNB1 being associated with a poor prognosis[37]. Data from The Human Protein Atlas indicate that approximately 40% of melanomas are negative for GNB1, while ~60% of cases exhibit weak to moderate expression of the protein (Supplementary Fig. 2). Given the
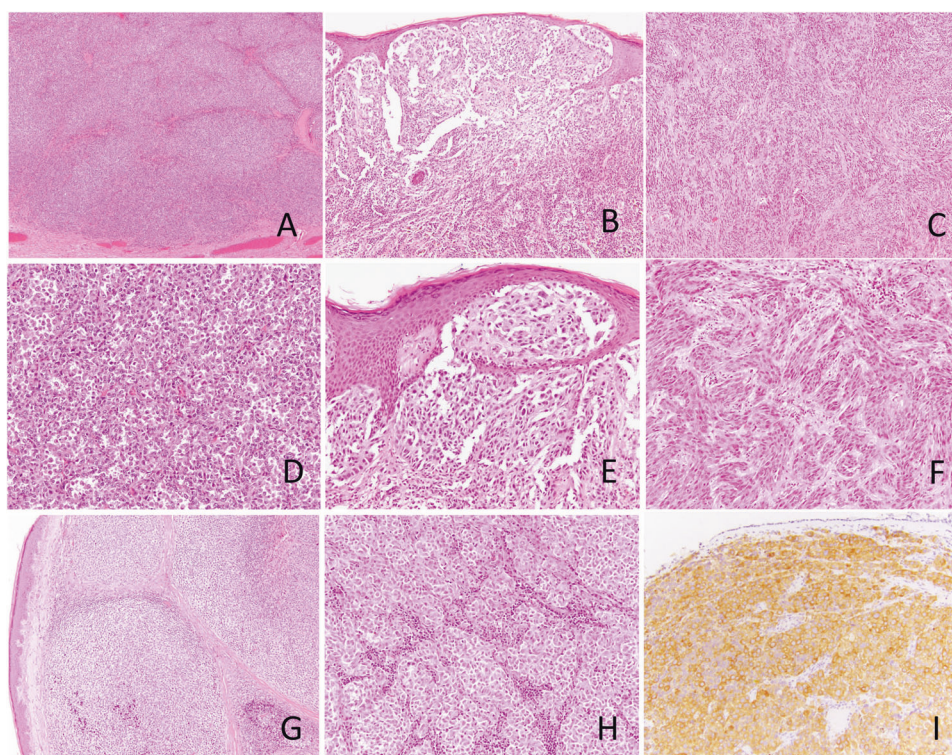
Fig. 4 Histology of fusion-positive melanomas. An epithelioid morphology is seen in melanomas with **A, D** *CANT1* (case 12), **B, E** *BRAF* (case 3), **C, F** *MAST2* (case 16), and **G** *NOTCH1* (case 14) fusions; whereas a spindle morphology is seen in a melanoma with **H** *RAF1* fusion (case 8). **I** ALK immunostain is strongly positive in the melanoma with *ALK* fusion (case 10).

strong, uniform distribution of GNB1 observed in the *NOTCH1::GNB1*-positive melanoma (Fig. 5C), we hypothesize that the rearrangement may be upregulating GNB1 expression in this tumor, under the control of the *NOTCH1* promoter.

MAST2 encodes a microtubule-associated serine/threonine kinase with anti-apoptotic properties, that is overexpressed in various tumors, including esophageal cancer, pancreatic cancer, and sarcomas[38]. In liver cancer, high expression of *MAST2* has been associated with advanced clinical stage and with a poor prognosis[39]. In addition, overexpression of a *MAST2* fusion detected in breast cancer had a proliferative effect on tumor cells[35]. The fusion described in that study had a different N-terminal partner from our melanoma case, but it involved the same *MAST2* breakpoint (exon 5) as the *NAGS::MAST2* rearrangement. We detected a similar pattern of MAST2 expression in the *NAGS::MAST2* -positive sample and in a *BRAF* V600E-mutant melanoma (Fig. 5E, F). Publically available datasets indicate that MAST2 is expressed in a subset of melanomas (Supplementary Fig. 3), suggesting that different tumors may induce MAST2 expression through different mechanisms. Taken together, our data suggest that the *NAGS::MAST2* fusion observed in case 16 may function as another mechanism to drive MAST2 expression.

BRAF fusions are common kinase translocations in tumors[40]. Although estimated to occur in 2.6%–6.7% of all melanomas, the frequency of *BRAF* fusions is higher in melanomas occurring in younger females and in Spitz neoplasms[23,41]. Four of our five *BRAF* fusion-positive tumors with available histologic sections exhibit an epithelioid morphology, not a spindled morphology, similar to previous report[25]. Treatment response to MEK inhibitor in a patient with *SKAP2::BRAF* fusion has been described in a recent case report[22]. Similarly, one of our patients with an *AGAP3::BRAF* fusion positive melanoma experienced a 30-month long response to trametinib. This is in contrast with a previously reported *AGAP3::BRAF* fusion that conferred resistance in cell lines to a BRAF inhibitor in a patient with melanoma[42]. High expression of a *BRAF*

fusion kinase has been shown to promote resistance to chemotherapy[41].

The presence of a *RAF1* fusion in melanocytic neoplasm is rare, occurring in less than 1% of neoplasms[40]. BRAF and CRAF, encoded by *RAF1*, form a heterodimer which activate the MEK-ERK pathway resulting in cell proliferation and survival[43]. Cell lines with *RAF1* fusions exhibit increased MEK phosphorylation in comparison to wild type[44]. RAF and MEK inhibitors may be useful in a subset of gene fusion-harboring solid tumors[12,19,21]. Excellent clinical responses were documented in 2 patients with *RAF1*-fusion melanomas following immunotherapy failure[19,21]. Four *RAF1* (*EFNB1::RAF1*, *LRCH3::RAF1*, *MAP4::RAF1*, *RUFY1::RAF1*) fusions were detected in four melanoma metastases in our series. In one patient, the same *RUFY1::RAF1* fusion was detected in two metastatic tumors. The patient was treated with a MEK inhibitor for four months. He experienced major response to therapy in his visceral organs but had marked progression in his bone metastases, possibly due to tumor heterogeneity or to impaired drug access to the bone lesions. Previously reported *RAF1* fusion partners include *AGGF1*, *ANO10*, *CDH3*, *CLCN6*, *CTDSPL*, *CTNNA1*, *GOLGA4*, *LMNA*, *LRCH3*, *LRRFIP2*, *MAP4*, *MPRIP*, *PAPD7*, *PRKAR2A*, *SASS6*, *SOX5*, and *TRAK1*[12,14,19,21,40,45–47]. Consistent with prior studies, the four melanomas with *RAF1* fusion were negative for pathogenic mutations in *BRAF*, *NRAS* and *NF1* (Fig. 1, Supplementary Table 2)[14,47]. *TERT* and *CDKN2A* concomitant mutations are frequently noted in the literature[14]. Similar to our findings, the majority of melanomas with *RAF1* fusion exhibit an epithelioid morphology[14].

ALK fusions are detected in 8–11%, 5–16% and 1–3% of Spitz nevi, atypical Spitz tumors and 1–3% Spitz melanomas, respectively[17,48]. Melanophilin (*MLPH*) gene was reported as partner gene to *ALK* in two Spitz nevi[49,50]. Echinoderm microtubule-associated protein-like 4 (*EML4*) is another partner gene to *ALK*[20,51]. Although the patient with the *EML4::ALK* fusion (case 10) did not respond to treatment with alectinib, a separate
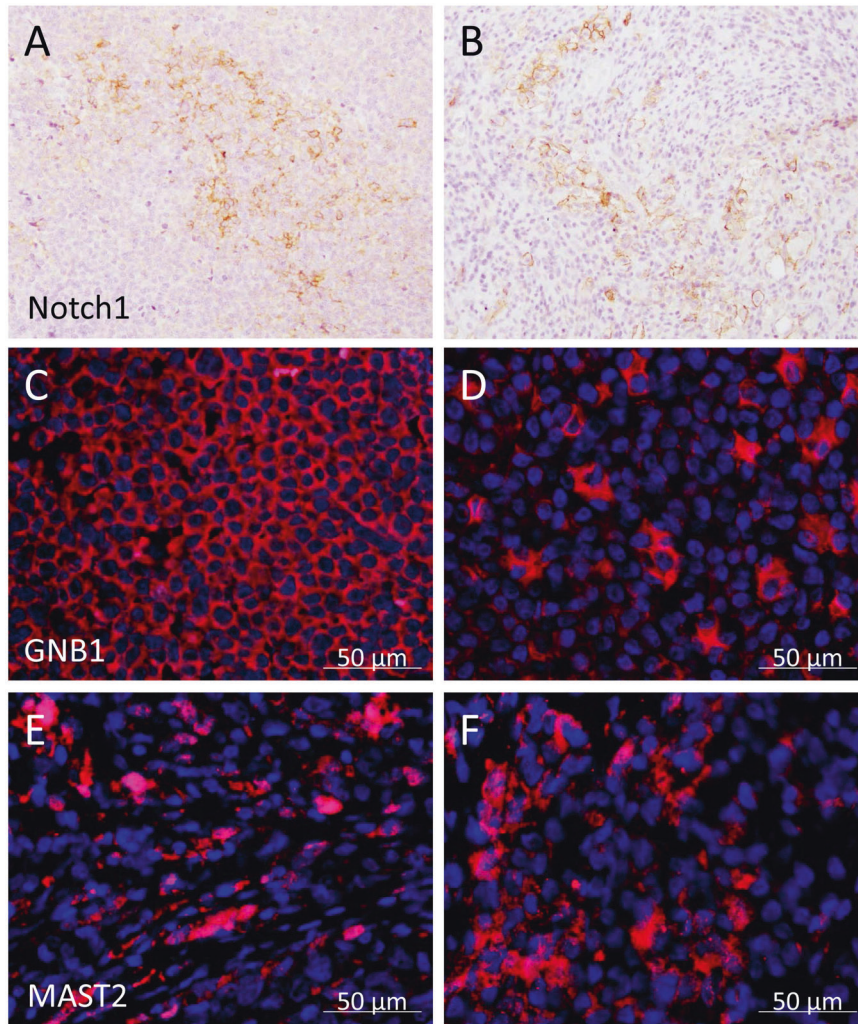
Fig. 5 Notch1 immunohistochemistry, and GNB1 and MAST2 immunofluorescence staining. Notch1 immunostains demonstrated similar levels of Notch1 protein expression in (**A**) a melanoma harboring a *NOTCH1::GNB1* rearrangement and in **B** a *BRAF* V600E-mutant melanoma. Immunofluorescence using a GNB1-specific antibody (**C**, **D**) detected uniform cytoplasmic and membranous GNB1 expression in (**C**) a melanoma harboring a *NOTCH1::GNB1* rearrangement (case 14), and heterogeneous distribution of GNB1 in (**D**) a *BRAF* V600E-mutant melanoma. Immunofluorescence using a MAST2-specific antibody (**E**, **F**) showed similar patterns of heterogeneous distribution of MAST2 protein in (**E**) a melanoma harboring a *NAGS::MAST2* rearrangement (case 16) and in (**F**) a *BRAF* V600E-mutant melanoma.

case report documented successful ALK inhibitor treatment for carcinoma with *EML4::ALK* fusion, suggesting the potential for ALK inhibitor use in melanoma[52].

TERT aberrations are detected most frequently in acral melanoma as compared with other melanoma subtypes[53]. In the fusion-positive melanomas in our series, *TERT* promoter mutation is the most frequent mutation identified, especially *TERT* 250 and *TERT* 228, followed by, recurrent inactivation of *CDKN2A*. Mutational analyses identified 14/15 triple wild-type tumors (negative for pathogenic mutations in *BRAF*, *RAS* and *NF1*) tumors.

Notably, nearly all tumors with gene fusions were *BRAF* and *RAS* wild-type (14/15; 93%) with one tumor with a *CCDC6::RET* fusion harboring two *BRAF* mutations *in cis*: the highly prevalent BRAF V600E mutation and a BRAF W604C variant of uncertain significance. It is unclear if, in this tumor, the proximity of the BRAF W604C variant affects the pathogenicity of the BRAF V600E mutation. Although concurrent *RET* fusions and *BRAF* mutations have been reported in papillary thyroid carcinoma (reported in 2.5–19.4% of tumors), gene fusions and *BRAF* and *NRAS* mutations are thought to be mutually exclusive in melanoma in the vast majority of cases[54]. Overall, our findings are consistent with previous literature that report that melanomas with fusions often

lack common driver mutations (*BRAF*, *RAS* and *NF1*)[13]. Gao et al. have investigated fusions in 9624 tumors of 33 different cancer types of The Cancer Genome Atlas (TCGA) cohort and reported that mutations were not found when fusion was already present in the same gene, supporting their mutual exclusivity in many malignancies[55]. We noted that, in our series, gene rearrangements were significantly enriched within the subset of triple wild-type melanomas that harbor *TERT* promoter mutations (18%). Since many cancer genotyping panels cover *BRAF*, *NRAS*, *NF1* and *TERT* promoter mutations, if a melanoma sample is "triple wild-type" and positive for a *TERT* promoter mutation, it may be worth testing it for gene rearrangements. In our cohort, 9 of those 10 (triple wild-type, *TERT*-mutant, fusion-positive) melanomas harbored a potentially actionable fusion. Identification of a fusion in such cases may be of critical importance as targeted therapy may provide an additional treatment option for clinicians. In our study, one patient with a *BRAF* fusion-positive melanoma experienced a durable response to treatment with a MEK inhibitor (case 1), while two other patients showed mixed responses to selective inhibitors (cases 9 and 10). Although more studies are needed to better understand the factors that regulate treatment effectiveness, the use of targeted

therapy has been reported to improve patient survival in some case reports[22].

In summary, we reported four novel fusions in melanomas: 2 fusions have been reported in other malignancies but not in melanoma and 2 have not been described in the literature. Our study shows a very strong correlation between the presence of a fusion and the lack of *BRAF/RAS/NF1* driver mutations, especially in *TERT* promoter-mutant melanomas. Detecting fusions in patients with advanced melanoma may have a clinically significant impact, especially in patients triple wild-type melanomas that harbor *TERT* promoter mutations, who have failed front-line immunotherapy.

DATA AVAILABILITY

All data generated or analyzed during this study are included in this published article and its supplementary information files.

REFERENCES

1. Matthews, N.H., Li, W.Q., Qureshi, A.A., Weinstock, M.A., Cho, E. Epidemiology of Melanoma. In: Ward WH, Farma JM, editors. Cutaneous Melanoma: Etiology and Therapy [Internet]. Brisbane (AU): Codon Publications (2017). Chapter 1. Available from: https://www.ncbi.nlm.nih.gov/books/NBK481862/ https://doi.org/10.15586/codon.cutaneousmelanoma.2017.ch1.
2. U.S. Cancer Statistics Working Group. United States Cancer Statistics: 1999–2010 Incidence and Mortality Web-based report. Atlanta, GA: Centers for Disease Control and Prevention, U.S. Dept of Health and Human Services and National Cancer Institute, National Institutes of Health (2013).
3. Chapman, P.B., Hauschild, A., Robert, C., Haanen, J.B., Ascierto, P., Larkin, J. et al. Improved survival with vemurafenib in melanoma with BRAF V600E mutation. *N. Engl. J. Med.* **364**, 2507–16 (2011).
4. Yang, K., Oak, A.S.W., Slominski, R.M., Brożyna, A.A., Slominski, A.T. Current molecular markers of melanoma and treatment targets. *Int. J. Mol. Sci.* **21**, 3535 (2020). https://doi.org/10.3390/ijms21103535.
5. Cancer Genome Atlas Network. Genomic Classification of Cutaneous Melanoma. *Cell.* **161**, 1681–1696 (2015).
6. Huang, F.W., Hodis, E., Xu, M.J., Kryukov, G.V., Chin, L., Garraway, L.A. Highly recurrent TERT promoter mutations in human melanoma. *Science.* **339**, 957–9 (2013).
7. Yan, X., Larsson, C., Xu, D. Mechanisms underlying the activation of TERT transcription and telomerase activity in human cancer: old actors and new players. *Oncogene.* **38**, 6172–6183 (2019).
8. Craig, S., Earnshaw, C.H., Virós, A. Ultraviolet light and melanoma. *J. Pathol.* **244**, 578–585 (2018).
9. Vergara, I.A., Wilmott, J.S., Long, G.V., Scoyler, R.A. Genetic drivers of non-cutaneous melanomas: challenges and opportunities in a heterogeneous landscape. *Exp. Dermatol.* **31**, 13–30 (2021).
10. Mertens, F., Johansson, B., Fioretos, T., Mitelman, F. The emerging complexity of gene fusions in cancer. *Nat. Rev. Cancer.* **15**, 371–81 (2015).
11. Yoshihara, K., Wang, Q., Torres-Garcia, W., Zheng, S., Vegesna, R., Kim, H., Verhaak, R.G. The landscape and therapeutic relevance of cancer-associated transcript fusions. *Oncogene.* **34**, 4845–54 (2015).
12. Palanisamy, N., Ateeq, B., Kalyana-Sundaram, S., Pflueger, D., Ramnarayanan, K., Shankar, S. et al. Rearrangements of the RAF kinase pathway in prostate cancer, gastric cancer and melanoma. *Nat. Med.* **16**, 793–798 (2010).
13. Turner, J., Couts, K., Sheren, J., Saichaemchan, S., Ariyawutyakorn, W., Avolio, I. et al. Kinase gene fusions in defined subsets of melanoma. *Pigment. Cell. Melanoma. Res.* **30**, 53–62 (2017).
14. Williams, E.A., Shah, N., Montesion, M., Sharaf, R., Pavlick, D.C., Sokol, E.S. et al. Melanomas with activating RAF1 fusions: clinical, histopathologic, and molecular profiles. *Mod. Pathol.* **33**, 1466–1474 (2020).
15. Forschner, A., Forschhammer, S., Bonzheim, I. NTRK gene fusions in melanoma: detection, prevalence and potential therapeutic implications. *J. Dtsch. Dermatol. Ges.* **18**, 1387–1392 (2020).
16. Quan, V.L., Panah, E., Zhang, B., Shi, K., Mohan, L.S., Gerami, P. The role of gene fusions in melanocytic neoplasms. *J. Cutan. Pathol.* **46**, 878–887 (2019).
17. Shaw, A.T., Gandhi, L., Gadgeel, S., Riely, G.J., Cetnar, J., West, H. et al. Alectinib in ALK-positive, crizotinib-resistant, non-small-cell lung cancer: a single-group, multicentre, phase 2 trial. *Lancet. Oncol.* **17**, 234–242 (2016).
18. Menzies, A.M., Yeh, I., Botton, T., Bastian, B.C., Scoyler, R.A., Long, G.V. Clinical activity of the MEK inhibitor trametinib in metastatic melanoma containing BRAF kinase fusion. *Pigment. Cell. Melanoma. Res.* **28**, 607–610 (2015).
19. Kim, K.B., Semrad, T., Schrock, A.B., Ali, S.M., Ross, J.S., Singer, M. et al. Significant clinical response to a MEK inhibitor therapy in a patient with metastatic melanoma harboring an RAF1 fusion. *JCO. Precis. Oncol.* **2**, 1–3 (2018).
20. Couts, K.L., Bemis, J., Turner, J.A., Bagby, S.M., Murphy, D., Christiansen, J. et al. ALK inhibitor response in melanomas expression EML4-ALK fusions and alternate ALK isoforms. *Mol. Cancer. Ther.* **17**, 222–231 (2018).
21. McEvoy, C.R., Xu, H., Smith, K., Etemadmoghadam, D., Leong, H.S., Choong, D.Y. et al. Profound MEK inhibitor response in a cutaneous melanoma harboring a GOLGA4-RAF1 fusion. *J. Clin. Invest.* **129**, 1940–1945 (2019).
22. Chew, S.M., Lucas, M., Brady, M., Kelly, C.M. SKAP2-BRAF fusion and response to an MEK inhibitor in a patient with metastatic melanoma resistant to immunotherapy. *BMJ. Case. Rep.* **14**, e238494 (2021). https://doi.org/10.1136/bcr-2020-238494.
23. Wiesner, T., He, J., Yelensky, R., Esteve-Puig, R., Botton, T., Yeh I. et al. Kinase fusions are frequent in Spitz tumours and spitzoid melanomas. *Nat. Commun.* **5**, 3116 (2014). https://doi.org/10.1038/ncomms4116.
24. Ferrara, G., Gianotti, R., Cavicchini, S., Salviato, T., Zalaudek, I., Argenziano, G. Spitz nevus, Spitz tumor, and Spitzoid melanoma: a comprehensive clinicopathologic overview. *Dermatol. Clin.* **31**, 589–598 (2013).
25. Kim, D., Khan, A.U., Compres, E.V., Zhang, B., Sunshine, J.C., Quan, V.L. et al. BRAF fusion Spitz neoplasms; clinical morphological, and genomic findings in six cases. *J. Cutan. Pathol.* **47**, 1132–1142 (2020).
26. Niu, H.T., Zhou, Q.M., Wang, F., Shao, Q., Guan, Y.X., Wen, X.Z. et al. Identification of anaplastic lymphoma kinase break points and oncogenic mutation profiles in acral/mucosal melanomas. *Pigment. Cell. Melanoma. Res.* **26**, 646–53 (2013).
27. Zheng, Z., Liebers, M., Zhelyazkova, B., Cao, Y., Panditi, D., Lynch, K.D. et al. Anchored multiplex PCR for targeted next-generation sequencing. *Nat. Med.* **20**, 1479–1484 (2014).
28. Li, H., Durbin, R. Fast and accurate short read alignment with Burrows-Wheeler transform. *Bioinformatics.* **25**, 1754–60 (2009).
29. Kent, W.J. BLAT – the BLAST-like alignment tool. *Genome Res* **12**, 656–64 (2002).
30. Thierauf, J., Ramamurthy, N., Jo, V.Y., Robinson, H., Frazier, R.P, Gonzalez, J. et al. Clinically integrated molecular diagnostics in adenoid cystic carcinoma. *Oncologist.* **24**, 1356–67 (2019).
31. Keung, E.Z., Gershenwald, J.E. The eighth edition American Joint Committee on Cancer (AJCC) melanoma staging system: implications for melanoma treatment and care. *Expert. Rev. Anticancer. Ther.* **18**, 775–784 (2018).
32. Hermans, K.G., Bressers, A.A., van der Korput, H.A., Dits, N.F., Jenster, G., Trapman, J. Two unique novel prostate-specific and androgen-regulated fusion partners of ETV4 in prostate cancer. *Cancer. Res.* **68**, 3094–8 (2008).
33. Kanedo, Y., Yoshida, K., Handa, M., Toyoda, Y., Nishihira, H., Tanaka, Y. et al. Fusion of an ETS-family gene, EIAF, to EWS by t(17;22)(q12;q12) chromosome translocation in an undifferentiated sarcoma of infancy. *Genes. Chromosomes. Cancer.* **15**, 115–121 (1996).
34. Celestino, R., Sigstad, E., Lovf, M., Thomassen, G.O.S., Groholt, K.K., Jorgensen, L.H. et al. Survey of 548 oncogenic fusion transcripts in thyroid tumours supports the importance of the already established thyroid fusions genes. *Genes. Chromosomes. Cancer.* **51**, 1154–1164 (2012).
35. Robinson, D.R., Kalyana-Sundaram, S., Wu, Y.M, Shankar, S., Cao, X., Ateeq, B. et al. Functionally recurrent rearrangements of the MAST kinase and Notch gene families in breast cancer. *Nat. Med.* **17**, 1646–1651 (2012).
36. Yoda, A., Adelmant, G., Tamburini, J., Chapuy, B., Shindoh, N., Yoda, Y. et al. Mutations in G protein beta subunits promote transformation and kinase inhibitor resistance. *Nature.* **21**, 71–5 (2015).
37. Cao, Y., Li, J., Jia, Y., Zhang, R., Shi, H. Circ RNA circ_POLA2 promotes cervical squamous cell carcinoma progression via regulating miR-326/GNB1. *Front. Oncol.* **10**, 959 (2020) https://doi.org/10.3389/fonc.2020.00959.
38. Eißmann, M., Schwamb, B., Melzer, I.M., Moser, J., Siele, D., Kohl, U. et al. A functional yeast survival screen of tumor-derived cDNA libraries designed to identify anti-apoptotic mammalian oncogenes. *PLoS. One.* **8**, e64873 (2013) https://doi.org/10.1371/journal.pone.0064873.
39. Jiao, Y., Li, Y., Jiang, P., Fu, Z., Liu, Y. High MAST2 mRNA expression and its role in diagnosis and prognosis of liver cancer. *Sci. Rep.* **9**, 19865 (2019) https://doi.org/10.1038/s41598-019-56476-x.
40. Stransky, N., Cerami, E., Schalm, S., Kim, J.L., Lengauer, C. The landscape of kinase fusions in cancer. *Nat. Commun.* **5**, 4846 (2014). https://doi.org/10.1038/ncomms5846.
41. Botton, T., Talevich, E., Mishra, V.K., Zhang, T., Shain, A.H., Berquet, C. et al. Genetic heterogeneity of BRAF fusion kinases in melanoma affects drug responses. *Cell. Rep.* **29**, 573–588 (2019).
42. Kulkarni, A., Al-Hraishawi, H., Simhadri, S., Hirshfield, K.M., Chen, S., Pine, S. et al. BRAF fusion as a novel mechanism of acquired resistance to Vemurafenib in BRAFV600E mutation melanoma. *Clin. Cancer. Res.* **23**, 5631–5638 (2017).
43. Lavole, H., Therrien, M. Regulation of RAF protein kinases in ERK signaling. *Nat. Rev. Mol. Cell. Biol.* **16**, 281–298 (2015).

44. Jones, D.T., Kocialkowski, S., Liu, L., Pearson, D.M., Ichimura, K., Collins, V.P. Oncogenic RAF1 rearrangement and a novel BRAF mutation as alternatives to KIAA1549:BRAF fusion in activating the MAPK pathway in pilocytic astrocytoma. *Oncogene*. **28**, 2119–2123 (2009).

45. Hayward, N.K., Wilmott, J.S., Waddell, N., Johansson, P.A., Field, M.A., Nones, K., et al. Whole-genome landscapes of major melanoma subtypes. *Nature*. **545**, 175–180 (2017).

46. Baltres, A., Salhi, A., Houlier, A., Pissaloux, D., Tirode, F., Haddad, V. et al. Malignant melanoma with areas of rhabdomyosarcomatous differentiation arising in a giant congenital nevus with RAF1 gene fusion. *Pigment. Cell. Melanoma. Res*. **32**, 708–713 (2019).

47. LeBlanc, R.E., Lefferts, J.A., Baker, M.L., Linos, K.D. Novel LRRFIP2-RAF1 fusion identified in an acral melanoma: a review of the literature on melanocytic proliferations with RAF1 fusions and the potential therapeutic implications. *J. Cutan. Pathol*. **47**, 1181–1186 (2020).

48. Wiesner, T., Kutzner, H., Cerroni, L., Mihm Jr, M.C., Busam, K.J., Murali, R. Genomic aberrations in Spitzoid melanocytic tumors and their implications for diagnosis, prognosis and therapy. *Pathology*. **48**, 113–31 (2016).

49. Chung, C.T., Marrano, P., Swanson, D., Dickson, B.C., Thorner, P.S. Fusion of ALK to the melanophilin gene MLPH in pediatric Spitz nevi. *Hum. Pathol*. **87**, 57–64 (2019).

50. Fujimoto, M., Togashi, Y., Matsuzaki, I., Baba, S., Takeuchi, K., Inaba, Y. et al. A case report of atypical Spitz tumor harboring a novel MLPH-ALK gene fusion with discordant ALK immunohistochemistry results. *Hum. Pathol*. **80**, 99–103 (2018).

51. Salari, B., Duncan, L.M., Lennerz, J.K., Holbrook, E.H., Emerick, K.S., Foreman, R.K. Observed progression from melanosis with melanocyte hyperplasia to sinonasal melanoma with distant metastasis and a unique genetic rearrangement. *J. Cutan. Pathol*. **48**, 948–953 (2021).

52. Sugiyama, K., Izumika, A., Iwakoshi, A., Nishibori, R., Sato, M., Shiraishi, K., et al. Successful Alectinib treatment for carcinoma of unknown primary with EML4-ALK fusion gene: a case report. *Curr. Oncol*. **28**, 1938–1945 (2021).

53. Liang, W.S., Hendricks, W., Kiefer, J., Schmidt, J., Sekar, S., Carpten, J. et al. Integrated genomic analyses reveal frequent TERT aberrations in acral melanoma. *Genome. Res*. **27**, 524–532 (2017).

54. Zhang, R., Dong, L., Yu, J. Concomitant pathogenic mutations and fusions of driver oncogenes in tumors. *Front. Oncol*. **10**, 544579 (2021). https://doi.org/10.3389/fonc.2020.544579.

55. Gao, Q., Liang, W.W., Foltz, S.M., Mutharasu, G., Jayasinghe, R.G., Cao, S., et al. Driver fusions and their implications in the development and treatment of human cancers. *Cell. Rep*. **23**, 227–238.e3 (2018).

AUTHOR CONTRIBUTIONS

COMPETING INTERESTS

The authors declare no competing interests.

ETHICS APPROVAL AND CONSENT TO PARTICIPATE

The study was conducted according to the guidelines of the Declaration of Helsinki, and approved by the Partners Human Research Committee, the institutional review board of Partners HealthCare (protocol code 2011P0001665).

ADDITIONAL INFORMATION

Supplementary information The online version contains supplementary material available at https://doi.org/10.1038/s41379-022-01138-z.

Correspondence and requests for materials should be addressed to Dora Dias-Santagata or Mai P. Hoang.

Reprints and permission information is available at http://www.nature.com/reprints